Reaction Mechanism of Cl-2 and 1-Alkyl-3-methylimidazolium Chloride Ionic Liquids

ARTICLE *in* THE JOURNAL OF PHYSICAL CHEMISTRY A · NOVEMBER 2011

Impact Factor: 2.69 · DOI: 10.1021/jp208095e · Source: PubMed

THE JOURNAL OF PHYSICAL CHEMISTRY A

ARTICLE

pubs.acs.org/JPCA

Reaction Mechanism of Cl_2 and 1-Alkyl-3-methylimidazolium Chloride Ionic Liquids

Shao-Wen Hu,* Zhu-Xiang Wang, Feng Qu, Tai-Wei Chu,* and Xiang-Yun Wang

Beijing National Laboratory for Molecular Sciences, Radiochemistry and Radiation Chemistry Key Laboratory of Fundamental Science, College of Chemistry and Molecular Engineering, Peking University, Beijing, 100871, China

Supporting Information

ABSTRACT: Systems containing 1-alkyl-3-methylimidazolium chloride ionic liquid and chlorine gas were investigated. Using relativistic density functional theory, we calculated the formation mechanism of trichloride and hydrogen dichloride anions in an $Emim^+Cl^- + Cl_2$ system. $Emim^+Cl_3^-$ forms without energy barriers. The more stable species $ClEmim^+HCl_2^-$ forms through chlorine substitution. Substitution of a H on the imidazolium ring is much easier than substitution on the alkyl side chains. Infrared, Raman, ESI-MS, and ^1H NMR spectra were measured for EmimCl, BmimCl, and DmimCl with and without Cl_2 gas. The coexistence of Cl_3^- and HCl_2^-, as well as chlorine-substituted cations, was confirmed by detection of their spectroscopic signals in the Cl_2 added ionic liquids. Cl substitution appears less serious for cations with longer side chains.

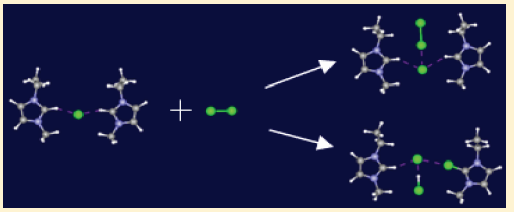

I. INTRODUCTION

Room temperature ionic liquid (IL) has been found to be an environmentally benign replacement for traditional molecular solvents in many areas.[1] The structure change of molecules and reactions happening in IL attract many investigations in recent years.[2] A typical IL is composed of a large organic cation and a small anion, such as *N*,*N*-dialkylimidazolium (Im^+) and halogen ion (X^-). Special interests were raised as halogen molecules were introduced into such an IL. In some cases, the ImX-based IL containing halogen-substituted cations were deliberately synthesized, because halogen-rich IL showed appealing physical properties such as high density and poor crystallizability.[3,4] In other cases, adding equivalent halogen molecules at 0 °C to some ImX, halogen substitution on the cation did not happen. Instead, trihalide anion X_2Y^- formed, in which the halogen atoms X and Y can be the same or different. It was found that the IL thus produced can be used as halogenation reagents.[5−9] Trihalide anions have been known for hundreds of years. Most of them can exist quite stably with large aprotic organic cations such as tetramethylamine in solid state.[10,11] It is, therefore, not surprising that trihalides can form in some large organic cation based ILs. Among the known trihalides, I_3^- is the earliest found one existing stably with alkali metal cation in aqueous solution and its numerous applications in many fields are still accumulating.[12] On the other hand, F_3^-, detected in recent years,[13−15] is apparently much more difficult to form and to exist stably in ordinary solvents. The intrinsic stability of trihalides in gas phase has been studied using theoretical[16−18] and experimental[19−22] methods. It is generally agreed that the binding energy of X_3^- in terms of equilibrium $X_2 + X^- = X_3^-$ (X = F, Cl, Br, I) is about 20−30 kcal/mol, which are quite large and close for different trihalides. Therefore, the actual order of stability for trihalides can hardly be explained by their binding energies in gas phase alone, but highly dependent on their surrounding species. In reality, the stability of trihalides was found $I_3^- > Br_3^- > Cl_3^-$ in aqueous solution but reversed the order in aprotic solvents.[23] Recently, the influencing effect of the surrounding proton on the stability of Br_3^- has been observed.[24]

In this work, our original intention was to find out the probable existence of Cl_3^- in ImCl-based IL, because we found Cl_2 is a good oxidizing reagent in the IL whereas Cl_3^- is not included in the reported Im-trihalides.[5] As we analyzed the results of electron spray ionization mass spectra (ESI-MS) for an ImCl + Cl_2 system, we found the signal of cations with one or two hydrogen atoms substituted by chlorine. If such substitution happens, HCl should be produced. In the system of HCl + EmimCl, hydrogen dichloride, HCl_2^-, has been detected.[25−27] The function of HCl_2^- in the proton transfer process of the ImCl-based IL has been studied using theoretical methods.[28] Thus, the following reactions may occur as Cl_2 is added to ImCl.

$$Cl_2 + Cl^- = Cl_3^-$$

$$Cl_2 + Im^+Cl^- = ClIm^+Cl^- + HCl$$

$$HCl + Cl^- = HCl_2^-$$

Understanding the mechanism of the reactions may give answers to three questions. (1) What happens as Cl_2 is added to ImCl. (2) How is the stability of Cl_3^- influenced by proton of the cation. (3) Whether can Cl_3^- and HCl_2^- coexist in the ImCl + Cl_2 systems.

Received: August 22, 2011
Revised: October 5, 2011
Published: October 11, 2011

Scheme 1. Numbering Order of the Atoms Composing $Emim^+$

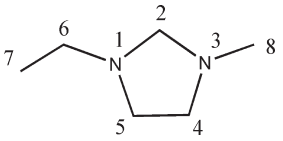

To our knowledge, as two hypervalent anions, the relationship of Cl_3^- and HCl_2^- has never been explored, although their structural similarities have been observed and studied comparatively quite early.[29,30]

For these reasons, we intended to study the reaction mechanism of $ImCl+Cl_2$ using density functional calculations in combination with several experimental techniques.

II. METHODS

1. Calculations. The geometry structures of all stationary points were fully optimized using the density functional with general gradient approximation (GGA) methods incorporated with all-electron basis set of valence triple-ζ plus two polarization functions (TZ2P). The systems are all regarded as ionic pairs, which involve only close-shell electronic structures. In such cases, spin−orbit interactions may be very small and its effects were not considered. For the heaviest atom chlorine, appearing as anion Cl^- in the IL, the relativistic effect may not be negligible. In addition, we are continuing our work on the similar systems containing heavier halogens and heave metals, in which relativistic effect are important. Therefore, in this work, the relativistic effect was considered and evaluated using scalar zero order regular approximation (ZORA). Frequency calculations using the same GGA method were performed to characterize their nature on the potential energy surface (PES) as well as to provide zero point vibration energy (ZPE), infrared (IR), and Raman spectra. Proton nuclear magnetic resonance (^1H NMR) shielding tensors for selected species were calculated using the same GGA incorporated with gauge-including atomic orbitals (GIAO) methods.[31−33] The chemical shifts (δ) were then calculated relative to a proper reference. Intrinsic reaction coordinate (IRC) calculations were performed for each transition state structure to ensure the correct connections between relevant reactant and product. Using each GGA optimized structure, single point calculation using hybrid density functional B3LYP incorporated with all-electron TZ2P basis set and scalar relativistic ZORA was performed. The final energies reported were at the hybrid B3LYP level with GGA calculated ZPE corrections. The energies calculated using the two methods were listed comparatively in Supporting Information, Table 1.

The interaction energy of molecular fragments in complexes was calculated and corrected by basis set superposition error (BSSE) and ZPE. This was referred to as binding energy (E_b). For all the energy items, the B3LYP calculated results were used except for ZPE, for which the GGA calculated results were used. The BSSE of two fragments in each complex were also listed in Supporting Information, Table 1.

ADF2007 program package[34] was employed for all the calculations. The accuracy criterion of 6.5 was used for all the numerical integration, which is a rough indication of the number of significant digits.

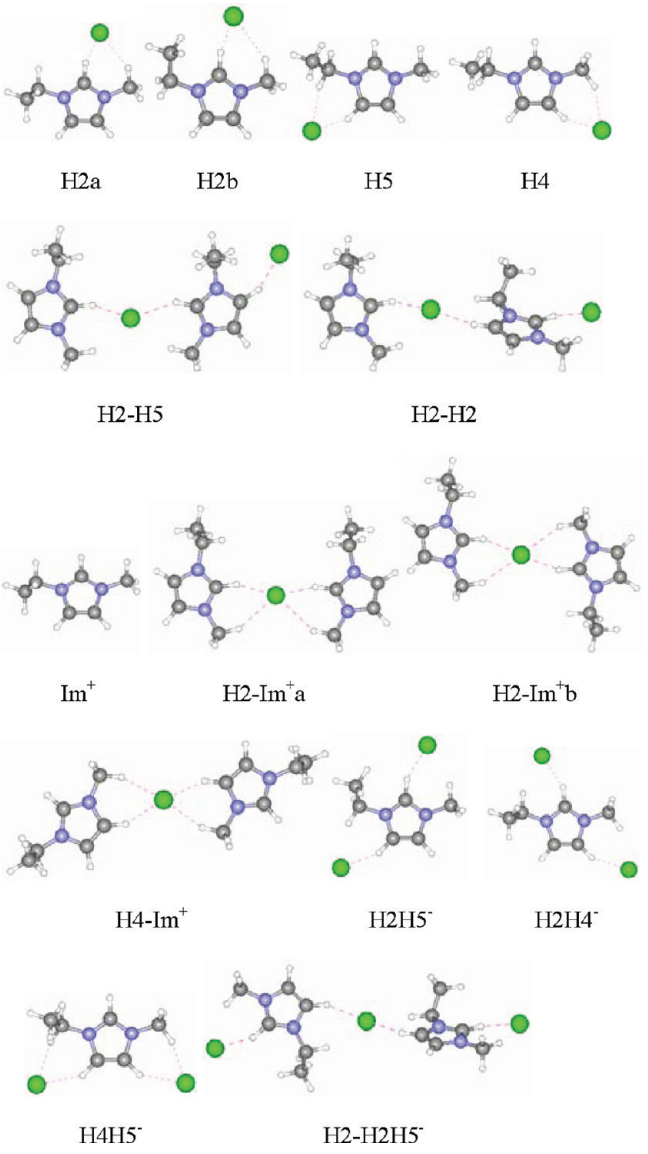

Figure 1. Optimized structure of the neutral and ionic fragments in EmimCl.

2. Experiments. The IL 1-ethyl-3-methylimidazolium chloride (EmimCl; >97%) was purchased from Sigma company. 1-butyl-3-methylimidazolium chloride (BmimCl; >99%), and 1-dodecyl-3-methylimidazolium chloride (DmimCl; >99%) were purchased from Lanzhou Institute of Chemical Physics, Chinese Academy of Sciences. All the ILs were used as received. Cl_2 was prepared by adding concentrated hydrochloric acid to solid $Ca(ClO_2)_2$. The resulting Cl_2 gas was then purified by passing through saturated NaCl and diluted H_2SO_4 solution, finally dried by concentrated H_2SO_4 and $Mg(ClO_4)_2$. Before reacting with Cl_2, the ILs were kept in a vacuum drying oven at 70 °C for 24 h. The Cl_2 gas was passed into 1 g of the IL sample kept in an oil bath at 70 °C for 30 min. During and after the reaction, the sample was wrapped with aluminum foil to avoid light and then stored in a desiccator to cool to room temperature before sending for spectroscopic measurements.

Infrared spectra were recorded on a Fourier transform spectrometer (Magna-IR 750, Nicolet) at wavenumbers 50−650 and 400−4000 cm^{-1}. Raman spectra were recorded on a Raman

Table 1. Relative Energy E_{rel} (kcal/mol), Binding Energy E_b[a] (kcal/mol), and Selected Infrared Spectra of the Species Shown in Figure 1

			wavenumber (IR intensity)			
species	E_{rel}	E_b	ν_{Cl-Im}	$\nu_{CH2-CH3}$	$\nu_{C-H\cdots Cl}$	$\nu_{C-H\cdots Cl}$
H2a	0.00	−93.49	191 (46)	220 (24)	2326 (1747)	2915 (160)
H2b	0.05	−93.32	188 (44)	224 (20)	2348 (1678)	2929 (130)
H5	8.14	−85.32	179 (61)	208 (4)	2637 (1067)	2830 (468)
H4	8.51	−85.05	181 (62)	209 (1)	2636 (1076)	2796 (621)
H2−H2	0.00	−10.72	185 (92)	216 (16)	2608 (1754)	2938 (161)
H2−H5	3.96	−14.90	182 (115)	215 (11)	2666 (1836)	2945 (154)
H2-Im$^+$a	0.00	−31.33	181 (122)	213 (13)	2818 (2215)	2967 (78)
H2-Im$^+$b	0.10	−31.22	179 (126)	211 (6)	2868 (2239)	3050 (97)
H4-Im$^+$	8.56	−31.24	176 (120)	209 (2)	2960 (1755)	3211 (34)
H2H5$^-$	0.00	−30.23	162 (107)	221 (1)	2784 (1035)	2843 (541)
H2H4$^-$	0.02	−30.20	165 (62)	205 (1)	2795 (977)	2890 (597)
H4H5$^-$	7.93	−30.64	142 (43)	208 (5)	2748 (526)	2984 (655)
H2−H2H5$^-$		−21.12	169 (235)	220 (1)	2700 (2343)	2989 (1337)

[a] E_b is ΔE of cation−anion association for single ion pairs; ΔE of two ion pairs association for ion-pair dimers; ΔE of association of the most stable neutral and ionic fragments for ionic species.

spectrometer (Ramanstation 400, PerkinElmer) at wavenumbers 100−2000 cm^{-1}. ^{1}H NMR spectra were obtained using a Bruker ARX-400 (400 MHz) spectrometer (Faellanden, Switzerland). Chemical shifts were given in ppm relative to tetramatheylsiliane (TMS) used as internal standard. ESI-MS spectra were measured on a high-resolution Fourier transform mass spectrometer (Bruker APEX IV FTMS, Faellanden, Switzerland).

III. RESULTS AND DISCUSSION

This section consists of two parts. In part I, we showed the calculated geometry structures, relative energies, and binding energies of some probable neutral and ionic fragments of EmimCl; revealed the reaction mechanism of Emim$^+$Cl$^-$ + Cl_2 by locating the reactants, intermediates, transition states, and products on the PES; and analyzed the bonding nature of Emim$^+$Cl$_3^-$ and Emim$^+$HCl$_2^-$. In part II, we compared the calculated spectroscopic data with IR, Raman, and ^{1}H NMR measurements and analyzed the ESI-MS ionization pattern and structures of fragments with the help of theoretical predictions.

The naming of the calculated species is as follows: For single ion pairs, Emim$^+$Cl$^-$, we use a H plus a number to indicate the closest cation−anion bond. For example, the name H2 means a single ion pair with anion Cl$^-$ closest to the H atom bonded to C2 (Scheme 1). For a Cl-substituted ion pair, ClEmim$^+$Cl$^-$, a name such as C4H2 means a Cl substitutes the H bonded to the C4 of the cation and the Cl$^-$ is closest to H2. For cations, Im$^+$ stands for Emim$^+$, C2$^+$ stands for ClEmim$^+$ with H2 substituted by Cl, and so on. For larger neutral or ionic fragments, the name is composed of two parts connected by a "−", indicating the easiest way to dissociate into smaller fragments, in consistence with the calculated binding energy. For the ion pairs containing Cl$_3^-$, the names are headed with an "R" to indicate they are regarded as reactants of the reaction pathways. For the intermediates, transition states, and products, "I", "TS", and "P", are added, respectively.

Part I: Theoretical Works

1. Neutral and Ionic Fragments of EimmCl. The structures of imidazolium-based ILs have been studied in detail using theoretical[35−37] and experimental[38,39] methods. The fundamental building blocks of EmimCl ionic liquid is ion pair Emim$^+$Cl$^-$ in several associated isomers. Three isolated ion pair isomers were located on the PES. Among these, species, H2 has two conformers, H2a and H2b, which differ in the ethyl side chain conformations. The number of such conformers would increase if the side chain becomes longer.[39] H2 are about 8 kcal/mol more stable than H4 and H5 due to a stronger H2$\cdots$Cl$^-$ interaction than H4$\cdots$Cl$^-$ or H5$\cdots$Cl$^-$ (Table 1). The bulk ionic liquid can be regarded as a hydrogen bonded network of these ionic pairs.[36] Taking two structures as examples, H2−H5 and H2−H2 are both an association of two ion pairs. H2−H2 is relatively low in energy whereas the binding energy of H2 and H5 in H2−H5 is larger. To interpret our ESI-MS measurements, we optimized the structure of several probable ionic fragments of EmimCl. The ionization may proceed along two channels. In one possible channel, EmimCl may dissociate into its building block or single ion pairs in the first step. The ion pairs then ionize into Emim$^+$ and Cl$^-$. This process needs to overcome a large cation−anion binding energy of about 80−90 kcal/mol. Under such high energetic condition, Emim$^+$ itself might decompose further into smaller fragments. The ionization of ImCl may follow another channel, ionizing directly into ionic fragments before dissociating into smallest neutral ion pairs. The ionization breaks weaker bonds while retains the stronger ones, resulting in relative stable ions. For EmimCl, if we assume the following ionization pattern

$$\text{H2}-\text{H2} + \text{H2}-\text{H5} = \textit{H2}-\textit{Im}^+\text{a} + \text{H2H5}^- + \text{H2a}$$

$$\Delta E = 49.80\ \text{kcal/mol}$$

The calculated ΔE is much less than E_b of single ion pairs, and the major smallest cation and anion of EmimCl should be H2−Im$^+$ and H2H5$^-$ or H2H4$^-$.

The larger ionic fragments may dissociate into smaller fragments in a second step ionization. Forming naked cation Im$^+$ needs to dissociate cations like H2−Im$^+$a, H2−Im$^+$b, or H4−Im$^+$. Such dissociation requires about 31 kcal/mol energy. On the other hand, dissociating H2H4$^-$, H2H5$^-$, and H4H5$^-$ into H2, H4, H5, and naked Cl$^-$ requires about 30 kcal/mol

energy. Therefore, the energy sufficient to produce Im^+ may also produce Cl^-. Larger anions, such as H2−H2H5$^-$, can be regarded as an aggregate of an ion pair H2 and anion H2H5$^-$, with a relatively small E_b (21 kcal/mol).

2. Formation of Emim$^+$Cl$_3^-$. Geometry optimization of a Emim$^+$Cl$^-$ + Cl_2 system leads to formation of Emim$^+$Cl$_3^-$ without energy barrier. Carefully choosing the relative positions of the cation and anion as initial structures prior optimization, we located nine minimum isomers (Figure 2). Five of them have H2···Cl$_3^-$ bond. The others contain H4···Cl$_3^-$ or H5···Cl$_3^-$ bond. The structure of the anion Cl$_3^-$ is almost linear. As an isolated anion, Cl$_3^-$ belongs to $D_{\infty h}$ symmetry group with two equal Cl−Cl bonds (Supporting Information, Table 1). The presence of cations causes the two Cl−Cl bonds different in length. The calculated two R_{Cl-Cl} are all slightly longer than the X-ray measured values for tetraphenylarsonium trichloride,[40] which are 2.227 and 2.305 Å. The difference of the two Cl−Cl bond lengths varies along with the strength of cation−anion interaction. Two kinds of binding energies were calculated for the isomers. For Emim$^+$Cl$_3^-$, E_{b1} is the binding energy of two neutral fragments, Cl_2 and Emim$^+$Cl$^-$. It varies from 13.16 to 15.20 kcal/mol, significantly lower than the E_{b1} of isolated Cl$_3^-$ (30.61 kcal/mol), which is the binding energy of Cl_2 and Cl$^-$. E_{b2} is the binding energy of Emim$^+$ and Cl$_3^-$. Comparing with the parameters of Emim$^+$Cl$^-$, we can see that R_{-+} is larger than R_{1Cl-H} and E_{b2} is smaller than E_b (Table 1). It appears that as Cl$^-$ becomes Cl$_3^-$, the cation−anion interaction becomes weaker. The result implies that, in the presence of cations, Cl$^-$ appears as a weaker electron donor and the strength of Cl$^-$ as an anion weakens as it associates with Cl_2.

3. Chlorine Substitution Reactions. Besides forming Cl$_3^-$, Cl_2 can associate with one of the ring carbon atoms of the cation through a weak Cl···C π bond, as shown in Figure 3 and Table 3, forming three transient intermediates, IC2, IC4, and IC5. The binding energies of Emim$^+$Cl$^-$ and Cl_2 in these local minima are close to zero after single point energy calculations at the B3LYP level and ZPE/BSSE corrections. A similarly weak π complex has been studied for organic electrophilic halogenation.[41] The π complexes are initial structures leading to ring substitution. Starting from IC2, bond breaking and forming processes happen simultaneously via transition state TSC2, at which the C2−Cl and Cl−H2 bonds partially form while Cl−Cl bond and C2−H2 bond partially break. The angle of the Cl−C2−H2 is close to 90°. Over a small energy barrier of 3.71 kcal/mol, the substitution completes. The immediate products should be ClEmim$^+$Cl$^-$+HCl.

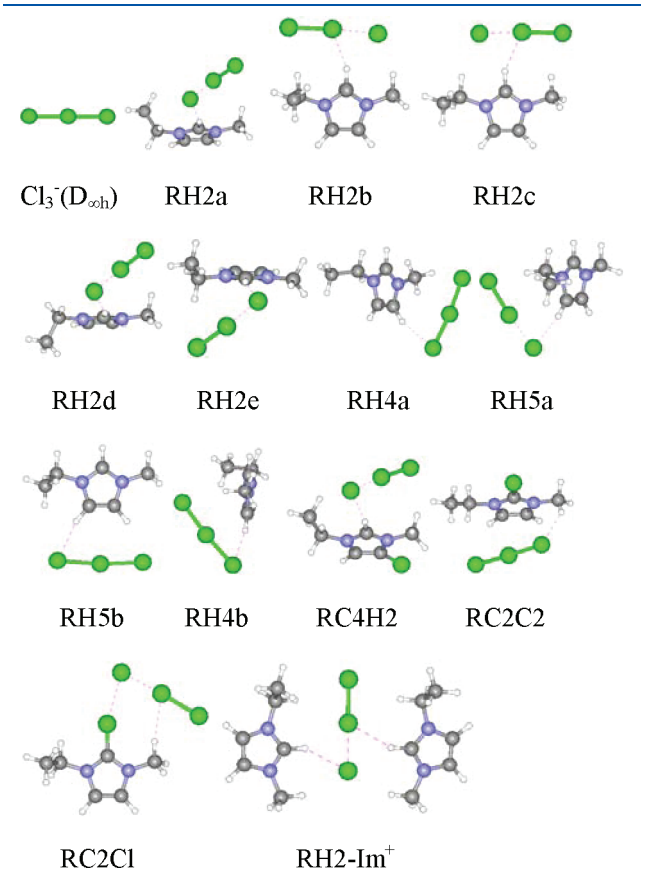

Figure 2. Optimized structure of the species containing Cl$_3^-$.

Table 2. Relative Energy E_{rel} (kcal/mol), Binding Energy E_b (kcal/mol), and Vibrational Spectra of the Species Shown in Figure 2

				wavenumber (IR, Raman)			
	E_{rel}	E_{b1}[a]	E_{b2}[a]	$\nu_{Cl-Cl-Cla}$	$\nu_{Cl-Cl-Cls}$	$\nu_{Cl-Cl-Clb}$	ν_{Cl3-Im}	ν_{C-H-Cl}
Cl$_3^-$			−30.61	281 (332, 0)	240 (0, 55)	149 (0.6, 0)		
RH2a	0.00	−13.40	−76.92	305 (217, 15)	232 (39, 21)	176 (0.5, 1.6)	129 (17, 1)	2967 (507, 134)
RH2b	0.05	−13.29	−76.85	299 (229, 9)	241 (27, 33)	180 (1.1, 0.1)	118 (23, 1.5)	3031 (430, 143)
RH2c	0.11	−13.25	−76.78	302 (239, 14)	238 (36, 31)	175 (0.2, 0)	124 (27, 1)	3038 (454, 157)
RH2d	0.12	−13.28	−76.79	305 (217, 16)	232 (42, 26)	176 (0.5, 2)	125 (21, 1)	2987 (376, 172)
RH2e	0.26	−13.16	−76.65	309 (177, 15)	230 (29, 15)	177 (0.4, 1.3)	123 (22, 2)	2991 (485, 152)
RH4a	6.66	−15.20	−70.30	295 (191, 1)	244 (18, 29)	184 (3, 1.5)	86 (3, 2)	3023 (363, 161)
RH5a	6.77	−14.73	−70.17	290 (170, 4)	243 (18, 36)	175 (0.3, 0.2)	119 (18, 1)	3003 (433, 161)
RH5b	6.80	−14.63	−70.10	285 (264, 1)	246 (4, 39)	182 (0.2, 0)	109 (33, 0.4)	3050 (393, 256)
RH4b	6.87	−14.98	−70.09	288 (135, 2)	246 (4, 38)	182 (3, 0.4)	106 (18, 0.7)	2991 (517, 228)
RC4H2	0.00	−12.58	−78.06	308 (207, 17)	232 (39, 27)	171 (3, 0.2)	128 (31, 2.5)	2945 (510, 93)
RC2C2	4.36	−15.18	−74.33	281 (205, 0.4)	243 (0.43, 35)	173 (2, 0.3)	99 (18, 0.7)	2941 (85, 221)
RC2Cl	12.67	−16.30	−66.61	295 (182, 13)	236 (33, 32)	174 (6, 3)	119 (47, 4.5)	3071 (40, 49)
RH2−Im$^+$		−7.56	−25.67	327 (176, 26)	224 (56, 16)	175 (0.1, 0.1)	119 (43, 3)	3112 (675, 116)

[a] E_{b1} is the binding energy of Cl_2 and the fragment of other parts; E_{b2} is the binding energy of cation and anion; for RH2-Im$^+$, E_{b2} is the binding energy of RH2b and Im$^+$.

dx.doi.org/10.1021/jp208095e |J. Phys. Chem. A 2011, 115, 13452–13466

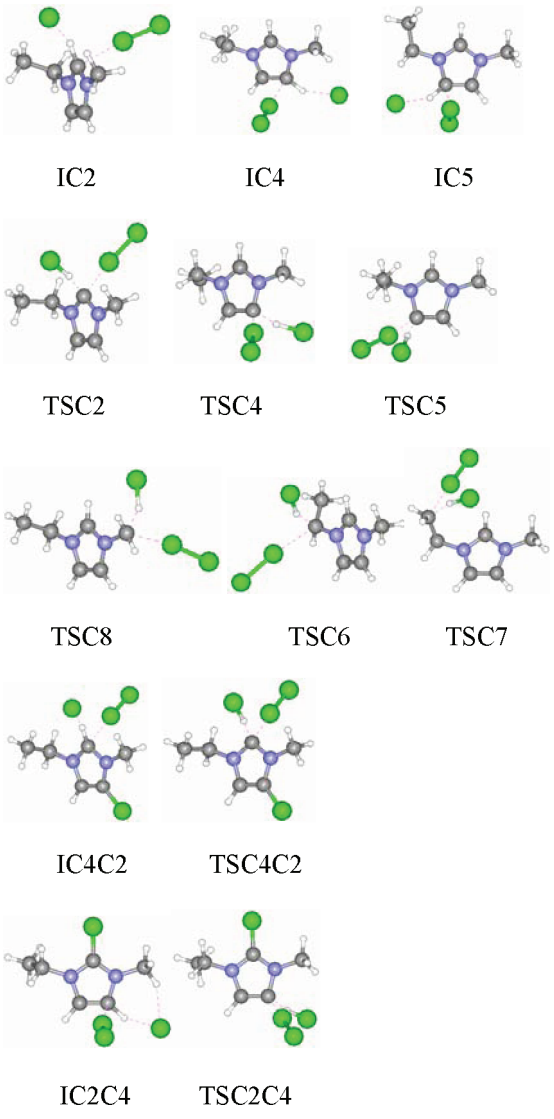

Figure 3. Optimized structure of transition states and transient intermediates in the substitution reaction of the $Emim^+Cl^-$ + Cl_2 and $ClEmim^+Cl^-$ + Cl_2 systems.

Along with the geometry optimization, however, HCl and Cl^- get closer and finally associate without energy barrier, leading to formation of PC2a (Figure 4), an ion pair composed of $ClEmim^+$ and HCl_2^-. The structure of IC2 is difficult to locate, a slight change in initial coordinate will lead to structure of RC2e (Figure 5a). Therefore, the reaction competes via two channels, forming RC2e without barrier or forming the more stable PC2a over a small barrier. Starting from IC4 or IC5, similar competes exist. The reaction leads to RC4a or RC5a without barrier, or leads to P4 or P5 via barriers slightly larger than that for C2 substitution. No intermediate species like IC2, IC4, and IC5 were located as initial structures for side chain substitution. On the PES, the located transition states TSC6, TSC7, and TSC8 are all high-energy saddle points connecting two low-energy minima. The large energy barriers may, therefore, prevent the side chain substitutions to realize.

Similar as Cl_3^-, the isolated HCl_2^- is also a linear symmetric anion with two equal H−Cl bonds. In the presence of cations, these bonds are different (Table 4) and the two R_{Cl-H} vary along

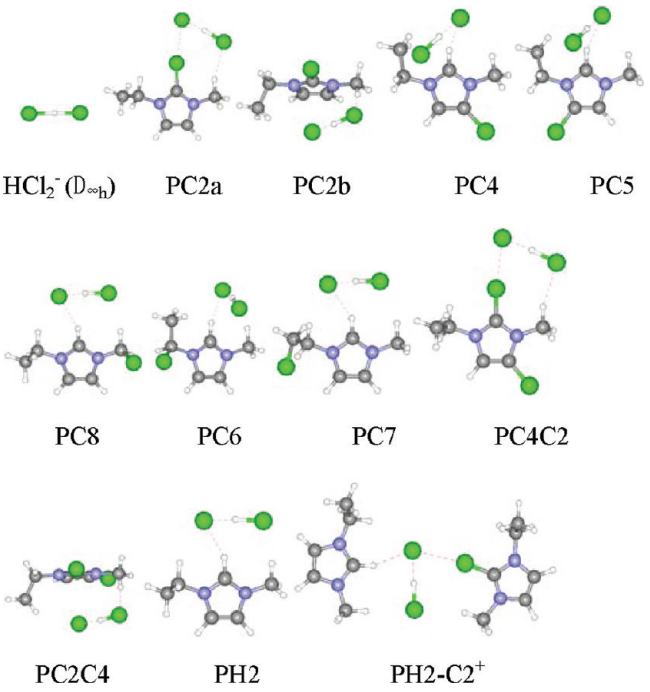

Figure 4. Optimized structure of the species containing HCl_2^-.

Table 3. Selected Bond Length (Å), Angle (Degree), and Activation Energy (kcal/mol) of the Species Shown in Figure 3

	R_{Cl-H}	R_{H-C}	R_{Cl-Cl}	R_{Cl-C}	A_{Cl-C-H}	E_a[a]
IC2	1.871	1.162	2.092	2.644	84.9	15.73
IC4	2.056	1.127	2.078	2.868	93.3	16.39
IC5	2.049	1.128	2.079	2.852	92.9	16.66
TSC2	1.530	1.394	2.204	2.232	87.9	3.71
TSC4	1.535	1.394	2.226	2.216	87.3	7.17
TSC5	1.537	1.394	2.214	2.246	86.1	7.21
TSC8	1.507	1.541	2.175	2.514	67.7	38.32
TSC6	1.500	1.582	2.181	2.555	64.6	39.58
TSC7	1.546	1.514	2.250	2.439	66.9	44.42
IC4C2	1.839	1.172	2.092	2.629	85.7	15.27
TSC4C2	1.524	1.399	2.191	2.257	88.1	3.05
IC2C4	2.007	1.135	2.071	2.896	92.6	22.51
TSC2C4	1.523	1.408	2.216	2.232	87.2	7.54

[a] E_a is defined as energy difference between transient intermediates and the reactants or transition states and intermediate. See Figure 5 for the connections.

with different cation−anion interactions. For the $ClEmim^+HCl_2^-$ systems, we also calculated two kinds of binding energy, which vary depending on the relative positions of the cation and anion. For the isolated HCl_2^-, the E_{b1} of HCl_2^- is considerable lower than that of Cl_3^-. For the ion pair $ClEmim^+HCl_2^-$, the E_{b1} and E_{b2} are influenced by the anion as well as by the Cl-substituted cation. To circumvent the substitution and evaluate the sole effect of Cl_3^- and HCl_2^- on E_{b2}, we choose to compare two structural analog species, RH2c and PH2. E_{b1} of PH2 is almost same as E_{b1} of RH2c, whereas R_{-+} is smaller and E_{b2} is larger for PH2. Therefore, compared to Cl_2, HCl associating to Cl^- has a less effect on cation−anion interaction.

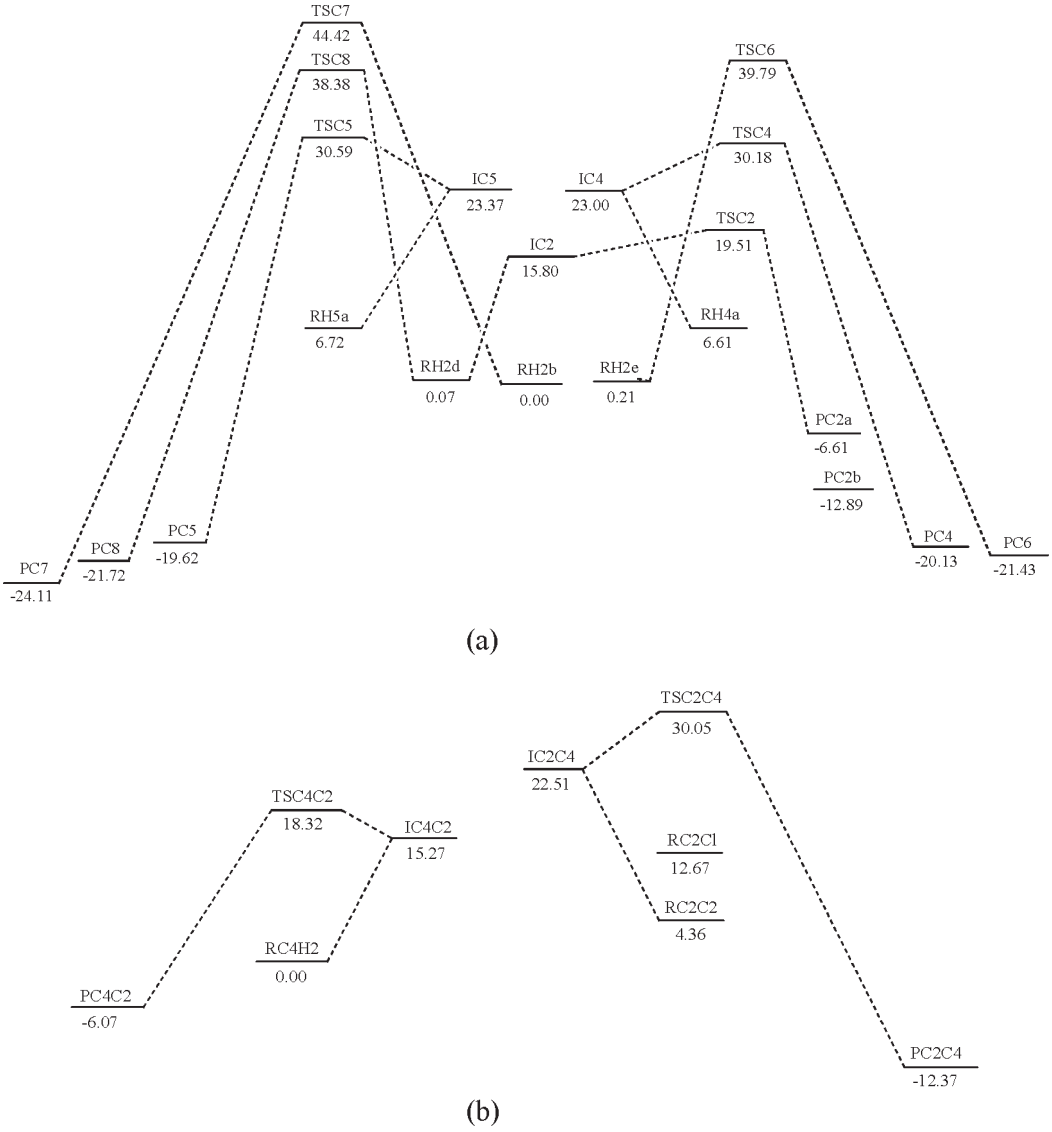

Figure 5. Substitution reaction channels and relative energy (kcal/mol) of $Emim^+Cl^-$ + Cl_2 (a) and $ClEmim^+Cl^-$ + Cl_2 (b).

Table 4. Relative Energy E_{rel} (kcal/mol), Binding Energy E_b (kcal/mol), and Vibration Spectra of the Species Shown in Figure 4

				wavenumber (IR, Raman)					
	E_{rel}	E_{b1}[a]	E_{b2}[a]	$\nu_{Cl-H-Cla}$	$\nu_{Cl-H-Cls}$	$\nu_{Cl-H-Clb}$	$\nu_{HCl2-Im}$	ν_{C-H-Cl}	ν_{C-Cl}
HCl_2^-			−25.50	965 (5026, 0)	314 (0, 9)	798 (7, 0)			
PC2a	0.00	−15.41	−70.29	1128 (2448, 257)	276 (49, 27)	838 (31, 0.6)	142 (67, 1)	2929 (136, 183)	435 (46, 96)
PC2b	−6.28	−12.36	−76.28	1084 (2320, 46)	293 (57, 2.5)	811 (75, 1)	81 (14, 1)	2891 (224, 272)	599 (65, 58)
PC4	−13.52	−12.51	−82.90	1252 (1631, 42)	271 (80, 3)	815 (100, 2)	121 (17, 0.5)	2881 (788, 146)	341 (5.5, 3)
PC5	−13.01	−12.17	−82.66	1264 (2009, 52)	269 (65, 5)	812 (92, 2)	122 (30, 0.4)	2896 (752, 153)	457 (9, 8)
PC8	−15.11	−12.48	−84.45	1172 (1354, 12)	298 (38, 1)	832 (88, 1)	147 (39, 1.4)	2947 (502, 181)	716 (114, 26)
PC6	−14.82	−10.41	−83.34	1363 (1809, 88)	255 (71, 3)	800 (94, 3)	121 (32, 0.3)	2858 (798, 77)	666 (34, 9)
PC7	−17.50	−14.42	−86.83	1271 (1284, 17)	271 (82, 2)	817 (79, 1)	136 (45, 0.2)	3014 (475, 142)	642 (31, 13)
PC4C2	0.00	−14.52	−70.68	1199 (3191, 452)	269 (29, 23)	831 (34, 1)	138 (65, 0.4)	2935 (130, 172)	367 (38, 79)
PC2C4	−6.30	−11.27	−76.65	1169 (2260, 81)	279 (64, 4)	803 (79, 1)	100 (21, 1)	2900 (205, 254)	599 (49, 78)
PH2		−13.09	−81.45	1205 (1970, 30)	277 (73, 3)	818 (61, 1)	140 (38, 0.2)	2963 (378, 467)	
PH2-$C2^+$		−10.87	−20.28	1378 (1388, 109)	255 (35, 8)	821 (21, 1)	145 (55, 2)	3006 (761, 377)	482 (6, 95)

[a] E_{b1} is the binding energy of HCl and the fragment of the other parts; E_{b2} is the binding energy of cation and anion; For PH2−$C2^+$, E_{b2} is the binding energy of PH2 and $C2^+$ (Supporting Information, Table 1).

dx.doi.org/10.1021/jp208095e |J. Phys. Chem. A 2011, 115, 13452–13466

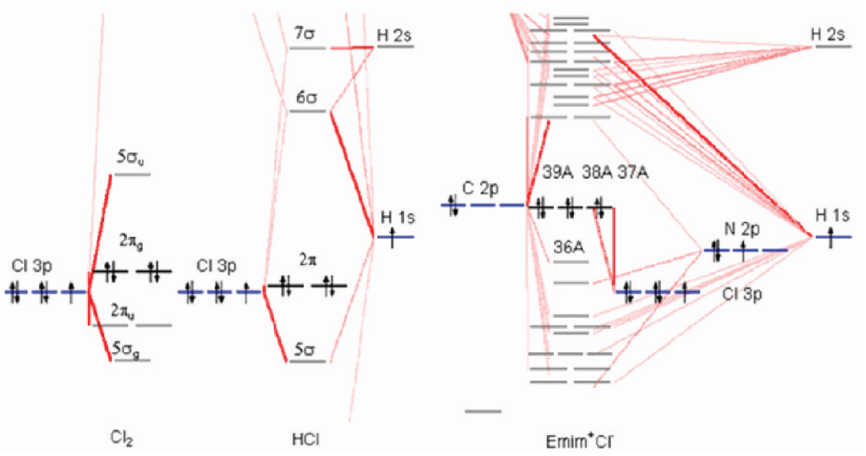

Figure 6. Energy level diagram of Cl_2, HCl, and $Emim^+Cl^-$.

Compared to $Emim^+Cl_3^-$, E_{b2} is lower for the species with C2 substitution. However, introducing an electron withdrawing atom Cl to the ring may stabilize the cation. As a result, PC2a and PC2b are more stable than RH2e. Introducing Cl to C4, C5 or side chains, clearly enhances the cation−anion interaction as well as stabilizes the system. Therefore, as summarized in Figure 5a, the Cl substitution produces thermodynamically more stable HCl_2^- containing species.

In real experiments, after the monosubstitution, ClEmimCl may continue to react with Cl_2. It is interesting to see what happens if the $ClEmim^+HCl_2^-$ reacts further with Cl_2. Based on our calculations, the following reactions are slightly exothermic. The equilibrium will favor the production of Cl_3^- containing species RC2Cl and RC2C2 (Figure 2) if Cl_2 is abundant.

$$PC2a + Cl_2 = RC2Cl + HCl \quad \Delta E = -0.90 \text{ kcal/mol}$$

$$PC2b + Cl_2 = RC2C2 + HCl \quad \Delta E = -2.94 \text{ kcal/mol}$$

To evaluate the probability of Cl double-substitution, we studied two probable pathways via locating the relevant reactant, RC4H2 and RC2C2 (Figure 2 and Table 2), intermediates, IC4C2 and IC2C4, transition states, TSC4C2 and TSC2C4 (Figure 3 and Table 3), and products, PC4C2 and PC2C4 (Figure 4 and Table 4). As summarized in Figure 5b, the second Cl substitution follows similar process as Cl monosubstitution. Starting from IC4C2, the second C2 substitution requires to overcome an energy barrier of 3.05 kcal/mol. Starting from IC2C4, the energy barrier for the second C4 substitution is 7.54 kcal/mol. Therefore, the probability of the Cl double substitution for EmimCl + Cl_2 is almost same as that of monosubstitution providing Cl_2 gas is sufficient.

4. Bonding Nature of Cl_3^- and HCl_2^-. As indicated by Landrum et al. in their theoretical work,[16] the bonding of X_3^- or HX_2^- can be viewed as donor−acceptor interaction between close-shell fragments, X_2 and X^- or HX and X^-. In this work, the electronic feature was studied using molecular orbital (MO) analysis. In Figure 6, some frontier MOs of Cl_2, HCl, and $Emim^+Cl^-$ are shown in terms of their composing atomic orbitals. The lowest unoccupied MO (LUMO) of Cl_2 is $5\sigma_u$, composed of the empty $3p_z$ orbitals of Cl atoms. The relative low energy of $5\sigma_u$ makes Cl_2 a good oxidizing agent or electron acceptor. As Cl_2 associates with electron donor Cl^-, charge transfer happens, resulting in Cl_3^-. The MO of Cl_3^- responsible for the charge transfer is 14σ (Figure 7). It is composed of the highest occupied MO (HOMO) of the donor (3p of Cl^-), the LUMO of the acceptor ($5\sigma_u$ of Cl_2) and a contribution from lower occupied MO of the acceptor ($5\sigma_g$ of Cl_2). Compared with Cl_2, the LUMO of HCl (6σ), composed of 1s and 2s orbitals of H and a smaller part of $3p_z$ orbital of Cl, is considerable higher in energy. As HCl and Cl^- associate, the MO responsible for the charge transfer is 10σ. Compared to 14σ of Cl_3^-, MO 10σ of HCl_2^- has higher energy and less contribution from 6σ, the LUMO of HCl, indicating less charge transfer from Cl^- to HCl. The LUMO of Cl_3^- and HCl_2^- are also different. The LUMO (15σ) of Cl_3^- has a large contribution from $5\sigma_u$ and thus has relative low energy, which makes Cl_3^- still an oxidizing agent. The LUMO of HCl_2^- has a large contribution of 7σ and thus has much higher energy, which makes HCl_2^- difficult to accept electrons.

In the presence of $Emim^+$, we assume $Emim^+Cl_3^-$ is an association of $Emim^+Cl^-$ and Cl_2; $Emim^+HCl_2^-$ an association of $Emim^+Cl^-$ and HCl. The energy level diagrams (Figure 8) show how the MO responsible for charge transfer is composed of the composing fragmental orbitals. For $Emim^+Cl^-$, the HOMO and two other MOs, 37A, 38A, and 39A, are essentially degenerate, mainly composed of 3p orbitals of Cl. The energies of the MOs are slightly higher than $5\sigma_u$ of Cl_2 but lower than 6σ of HCl, implying that $Emim^+Cl^-$ is a better electron donor for Cl_2 than for HCl. The MO of $Emim^+Cl_3^-$ responsible for charge transfer is 54A, slightly lower in energy than the HOMO. The charge-transfer MO of $Emim^+HCl_2^-$ is 47A, one of the three essentially degenerate HOMOs. Examine the composition of the two MOs we can see that the contribution of $5\sigma_u$ in 54A is larger than the contribution of 6σ in 47A, indicating the more effective charge transfer as $Emim^+Cl_3^-$ forms. For both MOs, the contributions

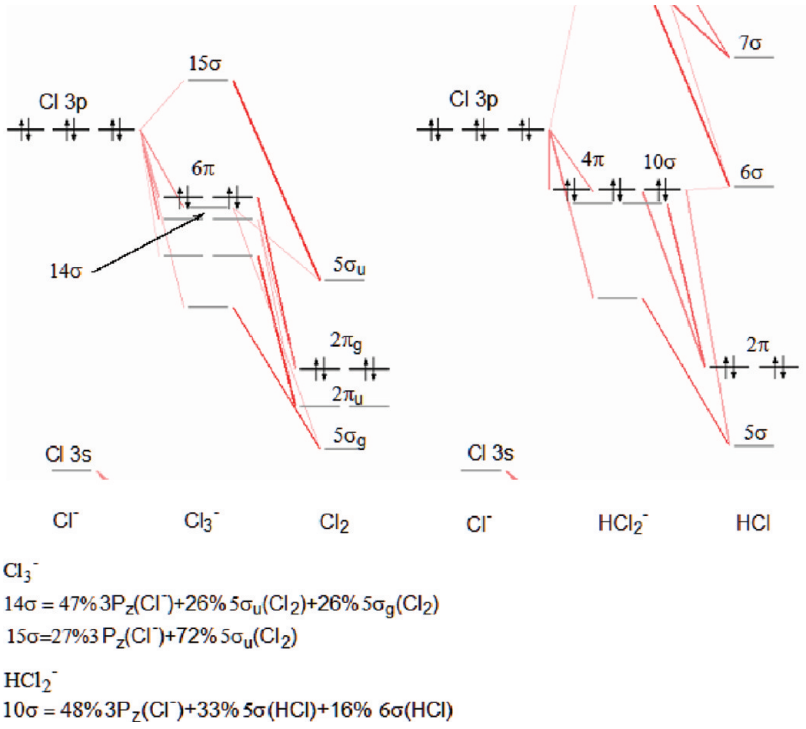

Figure 7. Energy level diagram of Cl_3^- and HCl_2^-.

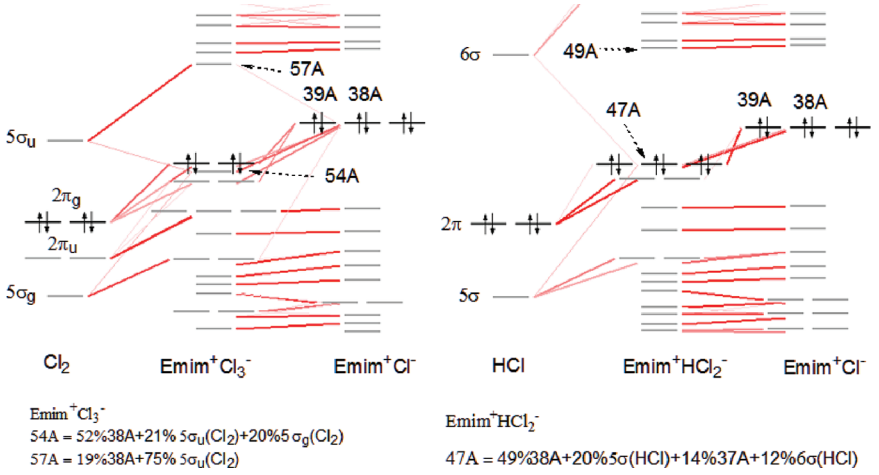

Figure 8. Energy level diagram of $Emim^+Cl_3^-$ and $Emim^+HCl_2^-$.

of acceptor's empty MOs are smaller than those in 14σ of Cl_3^- and 10σ of HCl_2^-, indicating the effect of the cation on the bonding. Besides the different contributions from the empty fragment orbitals, another difference between $Emim^+Cl_3^-$ and $Emim^+HCl_2^-$ is their LUMO. For the former, the LUMO 57A is composed of 75% 5σ_u of Cl_2, implying that $Emim^+Cl_3^-$ is an oxidant weaker than Cl_2. For the later, the contributions of LUMO 49A come mainly from the cation, implying that $Emim^+HCl_2^-$ can act as a weaker electron acceptor similar as Im^+.

Part II: Comparison of the Calculated Results with Experiments. *1. IR Spectra.* Measuring the absorption of species at IR region has been used to detect the existence of Cl_3^-[11,30,42] and HCl_2^-[25,43−45] in the presence of different cations. IR spectra has also been used to study the structure of ILs including ImCl.[39] According to our calculated results (Table 1), the IR spectra for fragments of EmimCl below 650 cm^{-1} show two feature peaks. One is the absorptions of Cl−Im stretching vibration (ν_{Cl-Im}) appear at 162−191 cm^{-1}, varies with the change of cation−anion interactions. The other is CH_3 rocking vibration, appearing at 205−224 cm^{-1}, too weak to be observed for some fragments. Both peaks can be vaguely identified in the measured spectra of EmimCl and BmimCl (Figure 9). For DmimCl, the rocking of CH_3 can not be singled out because the Cl−Im stretching peak appears at lower frequency region, perhaps due to longer cation−anion distance and weaker interactions caused by larger cation.

When Cl_2 is introduced into the systems, new bands appear at this region because Cl_3^- forms. Two kinds of Cl−Cl−Cl

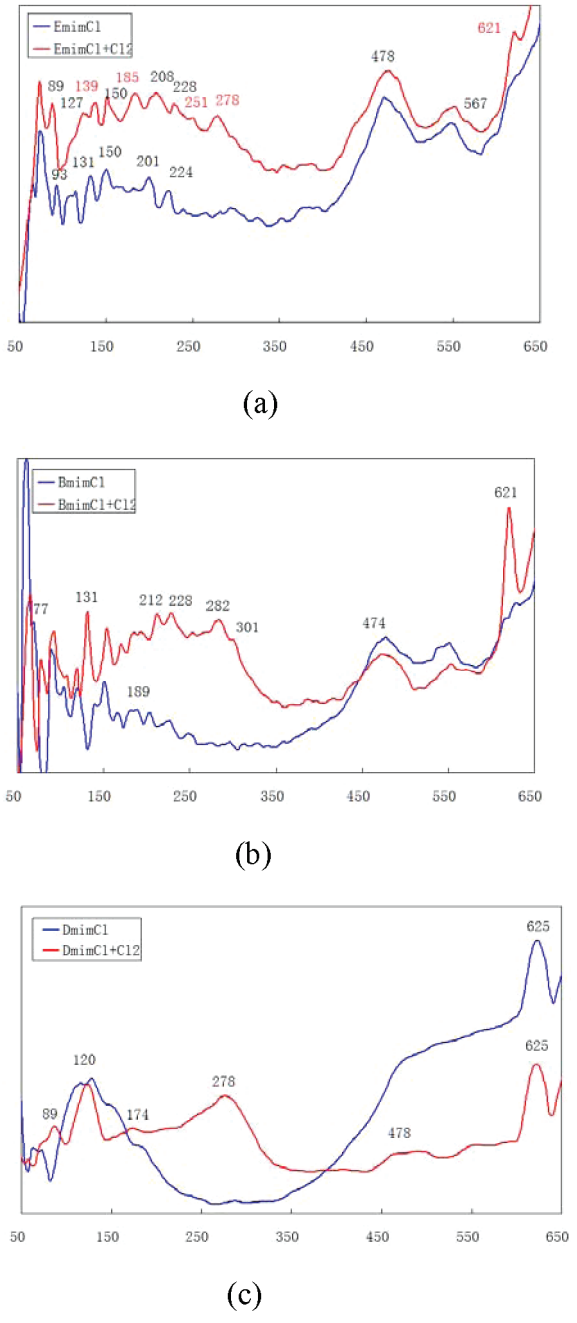

Figure 9. IR spectra of EmimCl (a), BmimCl (b), and DmimCl (c) with and without Cl_2 in 100−650 cm^{-1} region.

stretching modes (Scheme 2) cause absorptions at about 240−300 cm^{-1}. For isolated Cl_3^-, only Cl−Cl−Cla stretching mode ($\nu_{Cl-Cl-Cla}$) is IR active, the calculated absorption (Table 2) appears at 281 cm^{-1}. The bent mode ($\nu_{Cl-Cl-Clb}$) at 149 cm^{-1} is very weak. In the presence of $Emim^+$, the two Cl−Cl bonds of Cl_3^- are not the same, so the two stretching modes are both IR active. For the nine $Emim^+Cl_3^-$ isomers, the calculated $\nu_{Cl-Cl-Cla}$ at 285−309 cm^{-1} is stronger than the $\nu_{Cl-Cl-Cls}$ at 230−246 cm^{-1}. The measured IR spectra show a broad band peaked at 278, 282, and 278 cm^{-1} for EmimCl + Cl_2, BmimCl + Cl_2, and DmimCl + Cl_2, respectively, which were assigned to the Cl_3^- stretching modes. The formation of Cl_3^- weakens the cation−anion interaction. As a result, the band of Cl_3−Im

Scheme 2. Vibration Mode of Cl_3^- and HCl_2^-

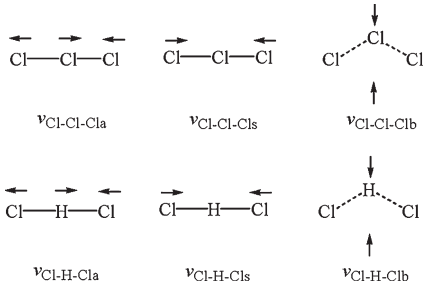

stretching (ν_{Cl3-Im}) appears at relative lower frequency than the band of ν_{Cl-Im} stretching for EmimCl. In Figure 9, the new band appears at 139 cm^{-1} for EmimCl + Cl_2, and the band at 131 cm^{-1} for BmimCl + Cl_2 may be caused by this effect.

For the Cl-substituted EmimCl, Cl_3^- can still exist. The Cl_3^- stretching modes are not influenced much by the substitution, as shown for the calculated species RC4H2, RC2C2, and RC2Cl (Table 2).

For isolated HCl_2^-, the symmetric stretching of HCl_2^- is not IR active. In the presence of cations, however, the two H−Cl bonds are different, so HCl_2^- has two IR active stretching mode (Scheme 2). According to the calculation (Table 4), Cl−H−Cls streching appears at 255−298 cm^{-1}, almost the same absorption region as for Cl_3^-, but considerably weaker.

In the IR spectra region from 600 to 4000 cm^{-1}, the calculated absorption band of asymmetric stretching vibration for isolated HCl_2^- appears intensively at 965 cm^{-1}; for species containing cations, the band appears at 1084−1363 cm^{-1}. The very weak band at 798 cm^{-1} is for isolated HCl_2^-, and for 800−838 cm^{-1} for species containing cations, is the absorption of HCl_2^- bent vibration. From the measured spectra (Figure 10), we can see that the broad new bands appears at 800−1700 cm^{-1} region. The new bands should be assigned to Cl−H−Cla streching, which has been shown as the typical absorption of HCl_2^-.[25] For EmimCl + Cl_2, the absorption of HCl_2^- is more intensive as the sample is exposed to light, implying the Cl substitution happens more serious at this condition. For DmimCl + Cl_2, the spectra change at this region is not large, implying the Cl substitution may not or less happens.

Another feature appears at higher frequencies, the absorption at about 3000 cm^{-1}, is the signal of C−H···Cl stretching. The calculated $\nu_{C-H\cdots Cl}$ of single ion pairs, H2, H4, and H5 is considerably smaller than the measured value (Figure 10). This is because the C−H bond weakens due to the presence of Cl^-, causing red shift of $\nu_{C-H\cdots Cl}$ vibration. This effect is strong for single ion pairs but weaker if Cl^- associates also with other cations. In reality, the IL is clearly not just single ion pairs, but a hydrogen-bonded net work. Consequently, the red shift is less for the measured bands. Adding Cl_2 to BmimCl, we can see that the absorption at this region decreases, but the frequency dose not change (Figure 10b). Adding Cl_2 to EmimCl, the absorption at this region decreases and also red shifts (Figure 10a). The red-shifted band appears more intensively as EmimCl + Cl_2 is exposed to light. Adding Cl_2 to DmimCl, the intensity and frequency does not change much in this region. According to our calculations, Cl substitution on one of the ring positions strengthens the H···Cl^- bond and weakens the C−H bond, resulting in a red shift of the strong absorption of C−H stretching. If the substitution happens only at the C2 position, the influence on C4−H

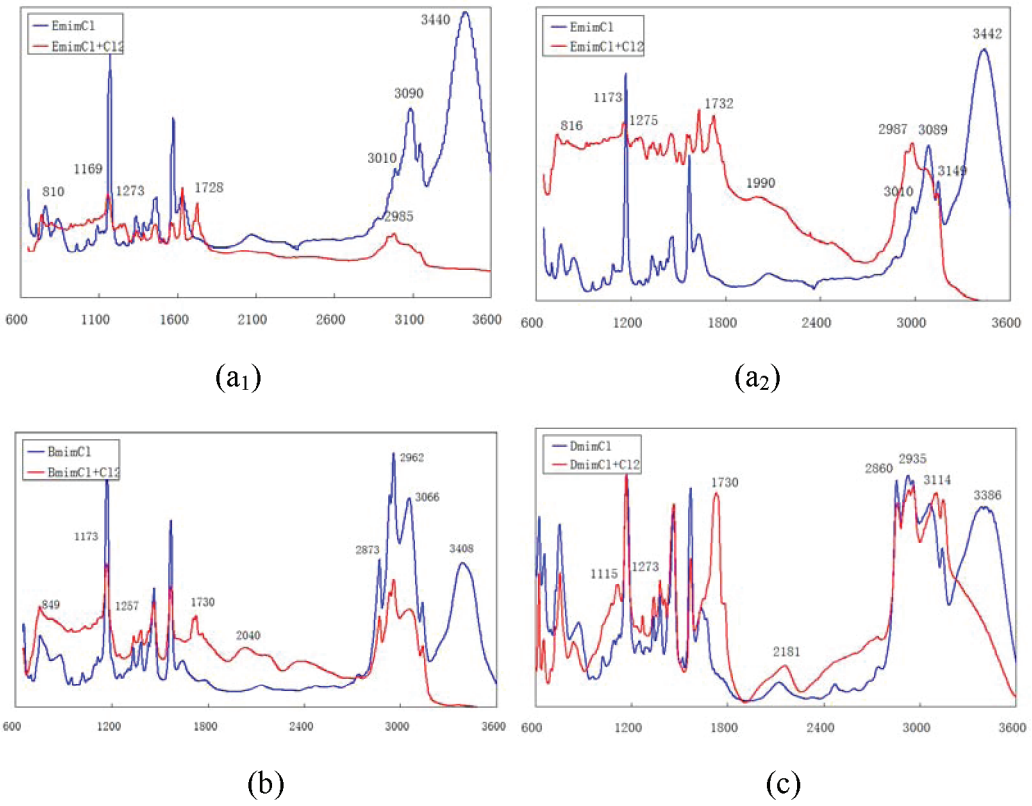

Figure 10. IR spectra of EmimCl (a_1), BmimCl (b), and DmimCl (c) samples kept in the dark; EmimCl (a_2) samples exposed to light with and without Cl_2 in the 600−3600 cm^{-1} region.

or C5−H stretching is small. Therefore, the partial C2 substitution effect appears as the intensity decreases (less C2−H bonds) rather than red shifts (weaker C2−H bonds). That is the case for BmimCl + Cl_2. For EmimCl + Cl_2, substitution is serious, and C4 or C5 substitution may also happen. The C2−H bond lengthens due to C4 or C5 substitution, resulting in a significant red shift of the C2−H stretching. For spectra of DmimCl + Cl_2, no significant changes in this region were observed. This perhaps indicates the least substitution upon adding Cl_2 to DmimCl.

The most significant spectroscopic feature after adding Cl_2 to the three IL systems is the disappearance of a band at about 3400 cm^{-1}. This band is assigned to the O−H stretching mode of H_2O. Possibly a small amount of H_2O associates with Cl^- in the original IL through a hydrogen bond. As Cl_2 is added to the IL, Cl^- associates with Cl_2 and H_2O is released and expelled as vapor. The interaction pattern and mechanism of H_2O releasing is not clear and worth further investigation.

2. Raman Spectra. Because Cl_3^- and H_2Cl^- are asymmetric in the presence of cations, their two kinds of stretching modes (Scheme 2) are both IR and Raman active. In Figure 11a, c, and d, we showed the measured Raman spectra in the region of 100−1700 cm^{-1} for the three ILs, with and without Cl_2. Adding Cl_2 to the ILs clearly causes new absorption at about 276 cm^{-1}. The Raman absorption appears at the same region as IR. Figure 11b is the calculated Raman spectra for the two most stable ion pair isomers of $Emim^+Cl^-$ and $Emim^+Cl_3^-$ and H2a and RH2a (Figures 1 and 2; Tables 1 and 2). The calculated absorption peak of Cl_3^- appears at a lower frequency than the measured results. This is because, in reality, the IL is not an isolated single ion pair. The presence and interaction of other cations weakens the Cl−Cl_2 bond. As in RH_2−Im^+, the calculated Raman absorption at $\nu_{Cl-Cl-Cla}$ enhances and blue shifts to 327 cm^{-1}, closer to the streching absorption of Cl_2, while the $\nu_{Cl-Cl-Cls}$ weakens and red shifts to 224 cm^{-1}.

The calculated $\nu_{Cl-H-Cls}$ of isolated HCl_2^-, appearing at 314 cm^{-1}, is Raman active. In the presence of a Cl-substituted cation, $\nu_{Cl-H-Cls}$ red shifts due to a weaker Cl−HCl interaction. Although, for most isomers, the Raman intensity at this region is weak; two of them, PC2a and PC4C2, have rather strong absorption at 276 and 269 cm^{-1}, respectively. The two species (Figure 4) are energetically and structurally favored products of mono and double Cl substitution. So the measured Raman spectra probably have their contribution. In addition, the peak in the spectra of EmimCl + Cl_2 showed two shoulders at 348 and 434 cm^{-1}. The calculated ν_{C-Cl} is also Raman active and appears at 435 cm^{-1} for PC2a and 367 cm^{-1} for PC4C2, which consists well with the measured shoulder frequencies. The calculated frequency of $\nu_{Cl-H-Clb}$ is not Raman active for isolated HCl_2^-. In the presence of a cation, $\nu_{Cl-H-Clb}$ appears weak at 800−838 cm^{-1}. The observed new peak at 802 cm^{-1} after adding Cl_2 to the three IL can be assigned to the vibrating mode.

The calculated $\nu_{Cl-H-Cla}$ of isolated HCl_2^- is not Raman active. In the presence of cations, the absorption at about 1000 cm^{-1} is Raman active and quite intensive for some species. In the measured spectra, however, there are no significant changes in this region after Cl_2 is added. This is perhaps not as specific for HCl_2^- due to strong interference.

3. ESI-MS Spectra. Figure 12 is the ESI-MS full scan spectra of EmimCl. In the positive-ion mode, no signal of the naked cation $Emim^+$. An intensive peak appears at m/z = 257, which is the

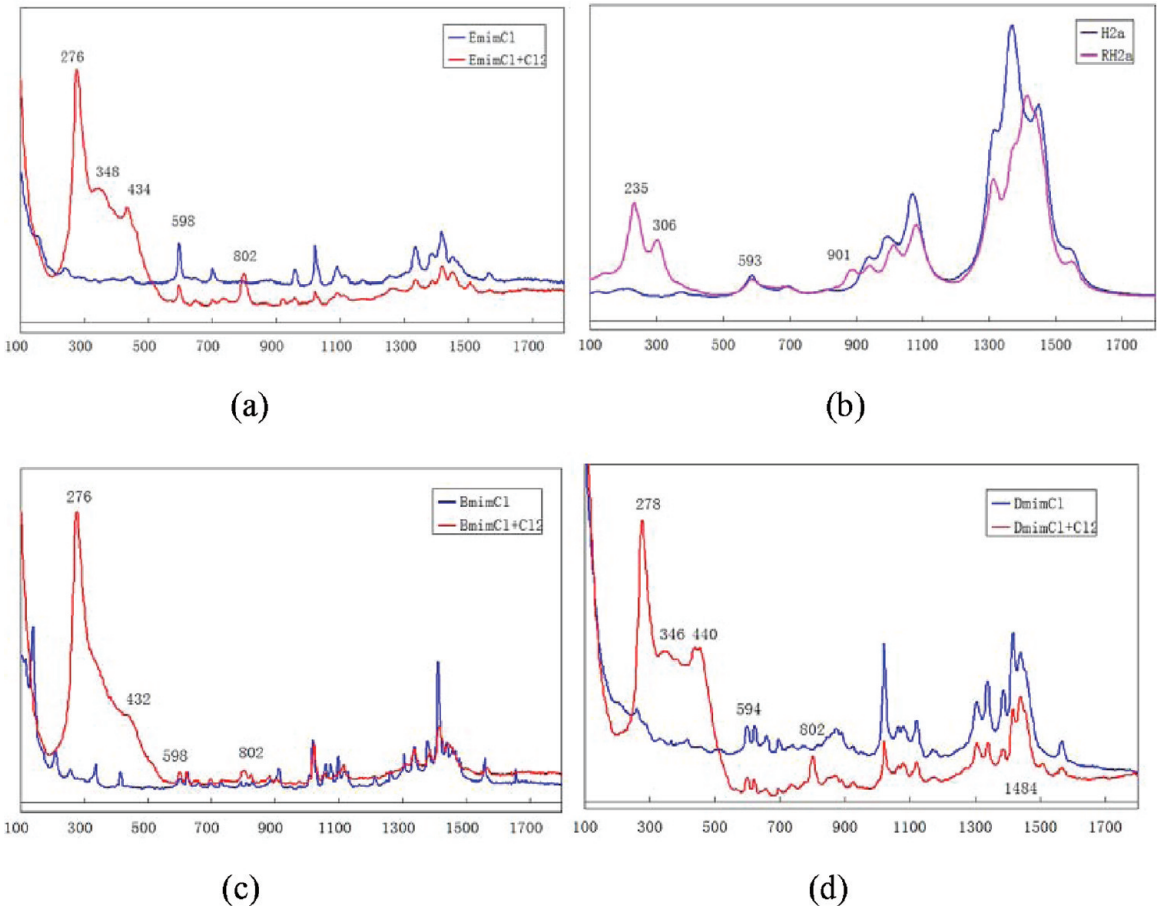

Figure 11. Raman spectra of EmimCl (a), BmimCl (c), and DmimCl (d), with and without Cl_2; Calculated Raman spectra of ion pairs $Emim^+Cl^-$ and $Emim^+Cl_3^-$ (b).

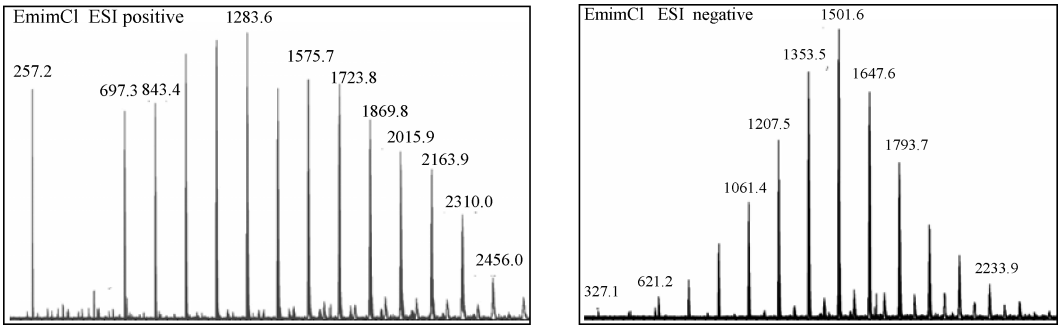

Figure 12. ESI-MS spectra of EmimCl.

signal of $Emim_2Cl^+$. It is the smallest cation formed during the ionization. According to our calculation, it should be the structure of H2−Im^+ (Figure 1) containing a relative strong H2···Cl···H2 interaction. The next intensive peak appears at m/z = 697, which is the signal of four ion pairs plus a $Emim^+$ or three ion pairs plus $Emim_2Cl^+$. It can be seen that the m/z values of larger aggregates increase by the number 146, which is the mass of one ion pair $Emim^+Cl^-$. In the negative-ion mode, the difference between each anion aggregate is also 146. Therefore, the ESI-MS spectra indicate that the cations and anions are both aggregates with different amounts of ion pairs. This picture supports our assumption that the IL is a hydrogen-bonded network of single ion pairs and the argument based on the calculations; ionization happens before the IL dissociates into single ion pairs. The cation $Emim_2Cl^+$ (m/z = 257) is especially stable so that the probability of second ionization into smaller fragments is negligible. Both $Emim^+$ and Cl^- were not detected. The signal of $Bmim^+$ (m/z = 139, Figure 13) is very small.

Our calculations predicted the formation mechanism of Cl_3^- and HCl_2^-. Their spectroscopic feature also detected in IR and Raman spectra. Cl_3^- has been detected in gas phase using MS method.[46] In our ESI-MS negative-ion mode, however, we did not detect the signal of the anions or any larger aggregates containing Cl_3^- or HCl_2^-. The calculated binding energy of Cl_2

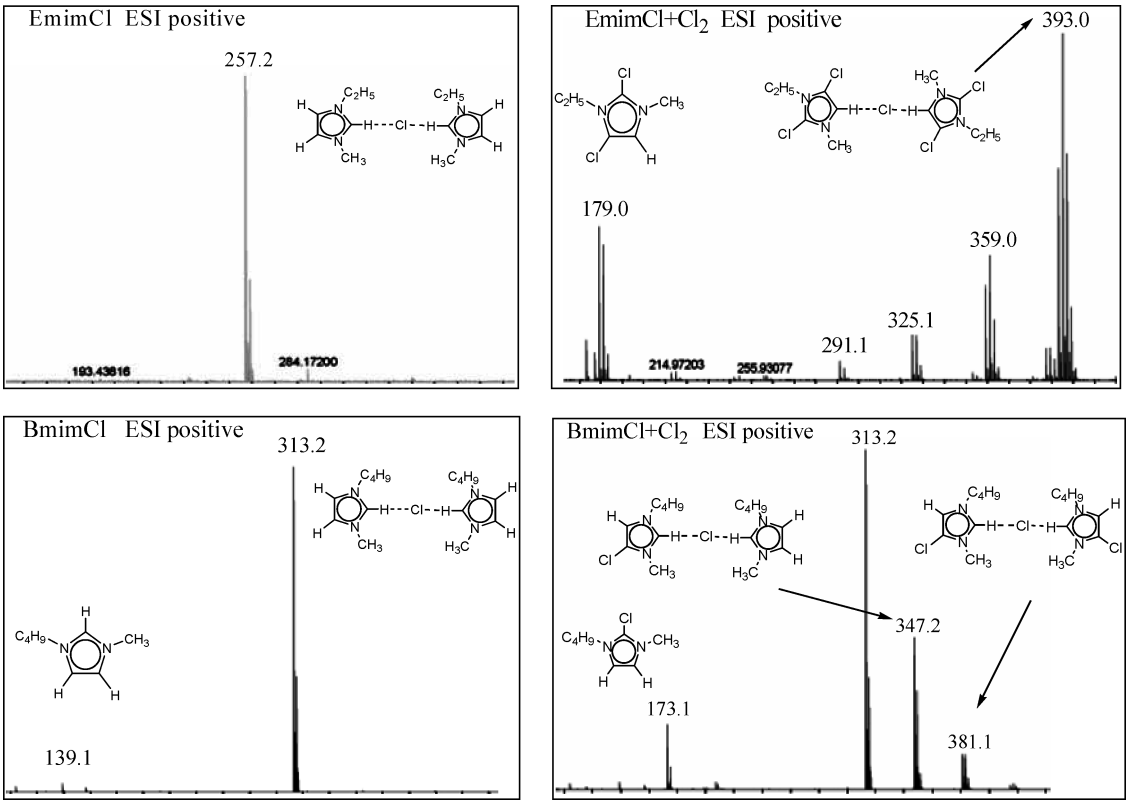

Figure 13. ESI-MS positive-ion mode of EmimCl and BmimCl with and without Cl_2.

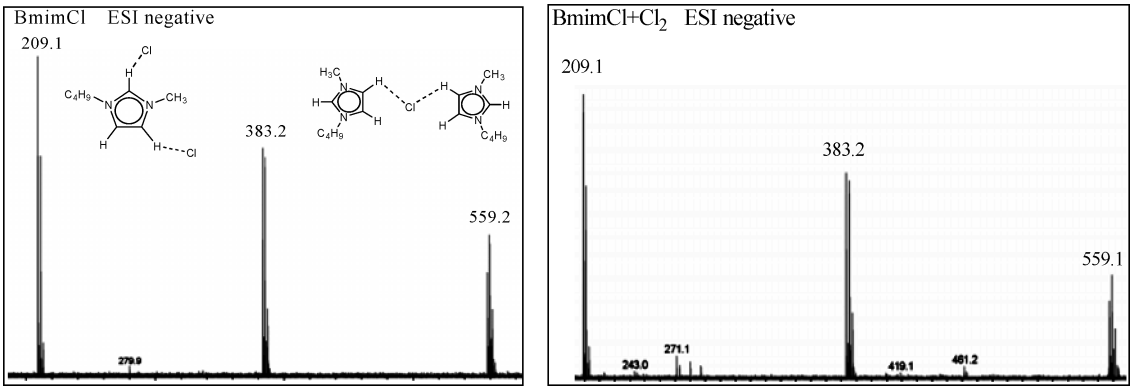

Figure 14. ESI-MS negative-ion mode of BmimCl with and without Cl_2.

and $Emim^+Cl^-$ (E_{b1}; Table 2) show that, for most $Emim^+Cl_3^-$, the E_{b1} is comparable with hydrogen bonds between ion pairs, such as H2−H5 (Table 1). In $Emim_2Cl_3^+$ (RH2−Im^+), however, the E_{b1} is only −7.56 kcal/mol. This implies that, as Cl^- associates with two $Emim^+$, its bonding with Cl_2 is much weaker. At the energetic condition of ionization, $Cl_2\cdots Cl^-$ bond is the weakest one and easy to break. That is perhaps the reason that Cl_3^- was not detected in our ESI-MS measurements. The result also implies that if adding Cl_2 to the IL simply results in $Emim^+Cl_3^-$, the original structure of the IL will not change significantly. Bortolini et al. have detected the signals of a series trihalide anion X_3^- and XY_2^- of the IL plus halogen molecules using ESI-MS measurement.[5] The missing of Cl_3^- in our work can be explained by two reasons. First, in their work, Cl_3^- is not included. It is possible that Cl_3^- shows different properties in terms of ionization compared with other trihalide anions. Second, the ionization conditions may be different. In the negative-ion mode spectra of their work, X^- appeared as intensive peaks. Therefore, a large part of the ion pairs was ionized into Im^+ and X^-. In this condition, halogen molecules can choose to associate with X^- to form X_3^- or XY_2^-. In our ESI-MS condition, the ionization is more "soft", no signals of isolated Cl^- appear in the negative-ion mode. $Cl_2\cdots Cl^-$ bond breaks before ionization and the dissociating pattern can still reflect the bonding nature of the original ILs. In general, the binding energy of HCl and Cl^- (E_{b1}, Table 4) in HCl_2^- is smaller than Cl_2 and Cl^- in Cl_3^-. So there are no signals of isolated HCl_2^- or larger aggregates containing the anion in the negative-ion mode spectra.

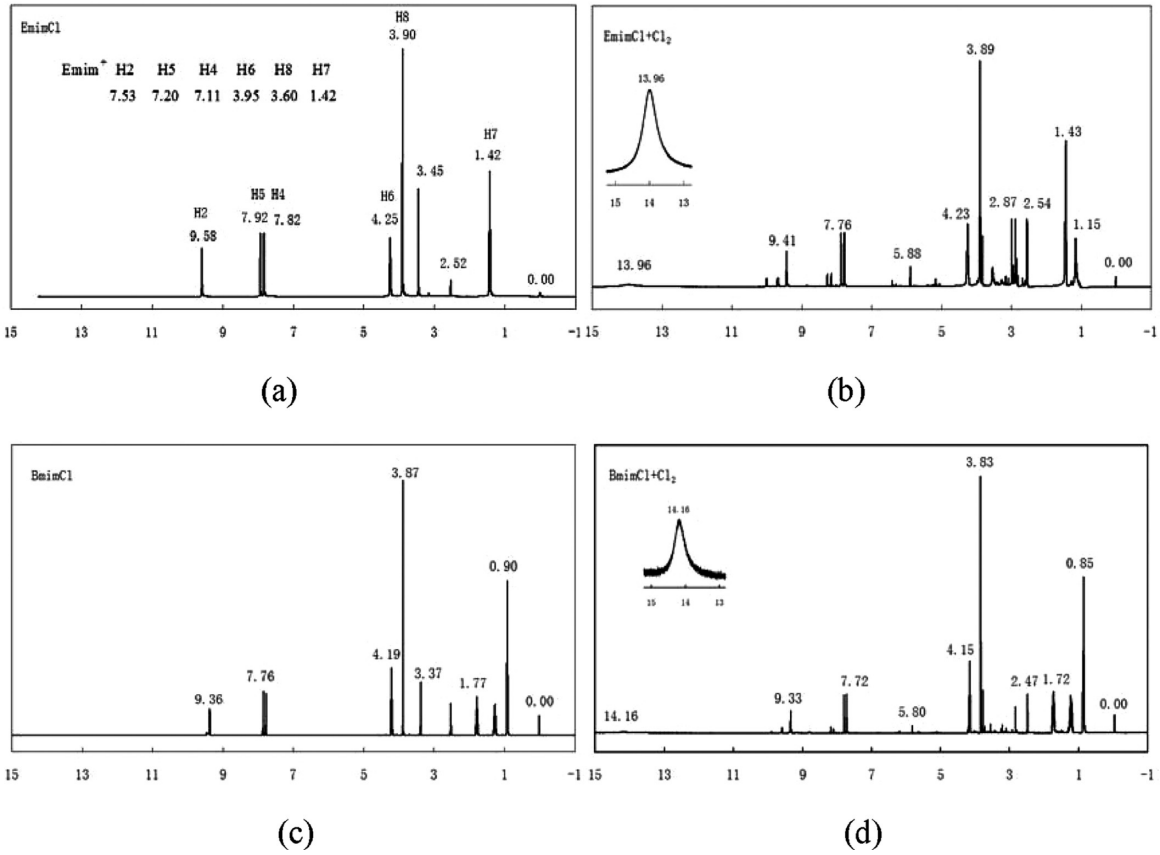

Figure 15. ^{1}H NMR spectra of EmimCl and BmimCl with and without Cl_2; the calculated δ for protons in the $Emim^+$ shown in a line in (a) with average δ = 1.42 for H7.

The signals of Cl-substituted cation were clearly recorded. It is quite difficult to control the extent of the substitution for the nonequilibrium systems. In general, keeping for a longer time and exposing to light cause the reaction to proceed more completely. For EimCl, substitution seems easier to happen than BmimCl. After adding Cl_2, the sample of EmimCl + Cl_2 was cooled overnight. The signal of the original $Emim_2Cl^+$, m/z = 257 in the positive-ion mode disappears. The major peaks are intensive signals of Cl double substituted cations m/z = 179 and 393 (Figure 15). Under similar conditions, the signals of BmimCl + Cl_2 are only those of Cl monosubstituted cations with m/z = 173, 347, and 381. The relative intensities of the signals are smaller than that of the nonsubstituted cation with m/z = 313, implying only a small part of BmimCl was substituted.

Unlike the positive-ion mode, the negative-ion mode spectra does not show signals of substituted anions for both ILs. As the H on the imidazole ring is substituted, forming an anion becomes difficult or less stable. As a result, the signals of negative-ion mode with and without Cl_2 are either not change for BmimCl (Figure 14) or not assignable for EmimCl (not shown). The results also support our calculated mechanism, substitution on the side chain is unlikely due to high energy barriers. Because if side chain substitution happened, there should be signals of $ClImCl_2^-$ in the negative-ion mode spectra.

4. ^{1}H NMR Spectra. Figure 15a,c is the measured ^{1}H NMR spectra of two ImCl. Because all the protons belong to the cation, the proton chemical shifts (δ) of the naked cation can be used as a reference to evaluate the effects of anions on the δ. The δ of H7 in EmimCl is the most upfield value least influenced by the ring and anions, so we took the calculated average δ of H7 to be the same as the measured value (1.42). The δ for other protons of $Emim^+$ was then calculated relative to the δ of H7, as shown in a line in Figure 15a. We can see that, except for proton H2, the calculated δ for all types of H of the cation is quite close to the measured values. It can be inferred that the presence of Cl^- may cause a significant change on the δ of H2 due to the relatively strong H2$\cdots$$Cl^-$ interaction. The δ of other protons does not change much with or without the Cl^-.

Addition of Cl_2 to the ImCl results in several new bands (Figure 15b,d). The new bands may be caused by three reasons. In the first place, the δ of the protons may change because of Cl substitutions. From our calculated results (Table 5), we can see that the effect of Cl substitution on the δ is quite small for the substitution occurred on the C2, C4, and C5 positions. The only large changes of δ appear on protons of the side chains with Cl substituting the H connected to the same carbon. This kind of substitution, however, is unlikely based on our mechanism study. Therefore, relatively large changes of δ may be caused by the second reason, new types of cation−anion interactions. The calculated changes of δ for all the protons as Cl_3^- and HCl_2^- form are listed in Table 6 for a few species that possess H2$\cdots$ anion type interactions. It can be seen that several large changes of δ occur at H2, H6, and H8. For H2, the formation of Cl_3^- causes δ to change 7−8 ppm upfield. This is because H2$\cdots$$Cl_3^-$ interaction is weaker than the H2$\cdots$$Cl^-$ interaction. The new band measured at 2.87 and 2.54 ppm (Figure 15b) may be caused

Table 5. Chlorine Substitution Effect on the ^{1}H NMR Chemical Shift of the Cations

	H2	H4	H5	H6	H6	H7	H7	H7	H8	H8	H8
Im^+	0.00	0.00	0.00	0.00	0.00	0.00	0.00	0.00	0.00	0.00	0.00
$C2^+$		−0.14	−0.10	0.18	−0.13	−0.07	−0.13	−0.01	−0.06	−0.14	−0.16
$C4^+$	−0.07		−0.22	−0.06	−0.07	−0.02	−0.02	−0.03	−0.08	−0.14	−0.15
$C5^+$	−0.08	−0.20		0.19	−0.12	0.06	−0.07	−0.19	−0.06	−0.04	−0.09
$C7^+$	−0.01	0.01	−0.06	0.05	0.04	1.87	2.08		0.00	0.01	0.01
$C8^+$	0.18	0.15	0.00	0.01	0.03	0.05	0.04	0.08	1.77	1.76	
$C6^+$	0.08	0.00	0.32	1.90		0.57	0.58	0.35	0.01	0.03	0.00
$C2C4^+$			−0.25	0.18	−0.20	−0.06	−0.15	−0.02	0.53	−0.50	−0.52

Table 6. Changes of ^{1}H NMR Chemical Shift as $Emim^+Cl_3^-$ and $ClEmim^+HCl_2^-$ Forms

	H2	H4	H5	H6	H6	H7	H7	H7	H8	H8	H8
H2a	0.00	0.00	0.00	0.00	0.00	0.00	0.00	0.00	0.00	0.00	0.00
RH2a	−7.55	0.15	0.15	0.78	0.03	0.28	0.01	0.02	−2.11	0.94	0.25
RH2b	−8.33	0.18	0.21	2.07	0.01	0.09	0.24	−0.03	−0.89	0.26	0.25
RH2c	−8.29	0.01	0.26	2.29	−0.06	0.02	0.06	0.01	−1.37	0.39	0.37
RH2d	−7.72	0.14	0.12	1.32	0.00	−0.18	0.07	0.07	−2.11	0.90	0.26
RH2e	−7.65	0.05	0.09	1.45	−0.10	0.85	0.18	0.03	−2.10	0.32	0.26
PC2a	16.87[a]	−0.01	−0.03	−0.01	−0.13	0.02	−0.07	−0.10	−0.11	0.09	0.08
PC2b	16.65[a]	0.04	0.12	−0.10	−0.06	1.89	−0.23	−0.30	−0.26	0.11	0.13

[a] Species with H2 becoming the proton of HCl_2^-, the reference is the same as the calcd δ in Figure 15a.

by the large δ change of H2. For H6, formation of Cl_3^- causes δ change about 2 ppm downfield due to the new type H6···Cl_3^- interaction. This change should be the source of the new band measured at 5.88 or 5.80 ppm (Figure 15b or d). For H8, formation of Cl_3^- causes δ change about 2 ppm upfield due to a weaker H8···Cl_3^- interaction. It is possible the source of the band appears at 1.15. These assignments, though quite vague, indicate that large δ change depends strongly on the surrounding anion rather than the change of the cation itself. The third reason to produce new bands is the formation of a new type of protons. For our systems, the products of Cl substitution contain one new type of proton in the anion HCl_2^-. Zawodzinski et al. have determined the ^{1}H NMR signal of HCl_2^- at δ = 13 ppm for an ImCl + HCl system.[27] In our ImCl + Cl_2 systems, we did observe the appearance of a small new band at about δ = 14 for EmimCl + Cl_2 and BmimCl + Cl_2 systems, which should be the signal of HCl_2^- produced during Cl substitution reactions. We also calculated the δ for two $ClEmimCl^+HCl_2^-$ ion pairs, PC2a and PC2b. Relative to our reference of δ = 1.42 for H7, the calculated δ is 16.87 and 16.65 for HCl_2^- in PC2a and PC2b, respectively. The discrepancy of the theory and experiment may come from the fact that we calculated isolated ion pairs, whereas, in actual cases, the ClH···Cl^- interaction may be weaker due to involvement of more cations.

Finally, the band detected at 3.45 (Figure 15a) or 3.37 (Figure 15c) ppm was assigned to the remaining H_2O in the ImCl. The bands disappear as Cl_2 was added to the ILs perhaps because the associated H_2O was driven away by the Cl_2 gas, in agreement with our observation on the IR spectra (Figure 13).

IV. CONCLUSIONS

EmimCl is a hydrogen-bonded network of single ion pairs $Emim^+Cl^-$. The H2···Cl^- interaction is strong so the formation probability of naked $Emim^+$ is small under mild ionization conditions. As Cl_2 is introduced to the IL, Cl_3^- forms without an energy barrier. The formation of Cl_3^- involves charge transfer from Cl^- to Cl_2 and thus weakens the cation−anion interaction of the IL. With the help of Cl^-, the Cl substitutions on the ring carbon especially on C2 happens over small energy barriers. The produced HCl then associates with Cl^- to form HCl_2^-. The formation of HCl_2^- also involves certain amount of charge transfer. The coexistence of Cl_3^- and HCl_2^- was evidenced by IR, Raman, and ^{1}H NMR spectra. The Cl substitution on C2 weakens the cation−anion interaction significantly. The Cl mono- or double-substituted single cation can, therefore, be easier observed using ESI-MS techniques.

■ ASSOCIATED CONTENT

Supporting Information. Supplemental Table 1 contains some calculated bond lengths and energies. This material is available free of charge via the Internet at http://pubs.acs.org.

■ AUTHOR INFORMATION

Corresponding Author
*E-mail: swhu@pku.edu.cn.

■ ACKNOWLEDGMENT

We are very grateful to the National Science Foundation of China (Grant No. 91026011) for financial support.

■ REFERENCES

(1) Welton, T. *Chem. Rev.* **1999**, *99*, 2071–2083.
(2) Ananikov, V. P. *Chem. Rev.* **2011**, *111*, 418–454.
(3) Mukai, T.; Nishikawa, K. *Solid State Sci.* **2010**, *12*, 783–788.
(4) Ye, Ch.; Shreeve, J. M. *J. Org. Chem.* **2004**, *69*, 6511–6513.

(5) Bortolini, O.; Bottai, M.; Chiappe, C.; Conte, V.; Pieraccini, D. *Green Chem.* **2002**, *4*, 621–627.
(6) Bagno, A.; Butts, C.; Chiappe, C.; Amico, F.; Lord, J. C. D.; Pieraccini, D.; Rastrelli, F. *Org. Biomol. Chem.* **2005**, *3*, 1624–1630.
(7) Dean, P. M.; Clare, B. R.; Armel, V.; Pringel, J. M.; Forsyth, C. M.; Forsyth, M.; MacFarlane, D. R. *Aust. J. Chem.* **2009**, *62*, 334–340.
(8) Cristiano, R.; Ma, K. F.; Pottanat, G.; Weiss, R. G. *J. Org. Chem.* **2009**, *74*, 9027–9033.
(9) Pavlinac, J.; Zupan, M.; Laali, K. K.; Stavber, S. *Tetrahedron* **2009**, *65*, 5625–5662.
(10) Chattaway, F. D.; Hoyle, G. *J. Chem. Soc., Trans.* **1923**, *123*, 654−662; DOI: 10.1039/ct9232300654.
(11) Evans, J. C.; Lo, G. Y-S. *J. Chem. Phys.* **1966**, *44*, 3638–3639.
(12) Zhdankin, V. V.; Stang, P. J. *Chem. Rev.* **2008**, *108*, 5299–5358.
(13) Ault, B. S.; Andrews, L. *J. Am. Chem. Soc.* **1976**, *98*, 1591–1593.
(14) Tuinman, A. A.; Gakh, A. A.; Hinde, R. J.; Compton, R. N. *J. Am. Chem. Soc.* **1999**, *121*, 8397–8398.
(15) Riedel, S.; Köchner, T.; Wang, X.; Andrews, L. *Inorg. Chem.* **2010**, *49*, 7156–7164.
(16) Landrum, G. A.; Goldberg, N.; Hoffmann, R. *J. Chem. Soc., Dalton Trans.* **1997**, 3605–3613.
(17) Bralda, B.; Hiberty, P. C. *J. Phys. Chem. A* **2008**, *112*, 13045–13052.
(18) Novoa, J. J.; Mota, F.; Alvarez, S. *J. Phys. Chem.* **1988**, *92*, 6561–6566.
(19) Nizzi, K. E.; Pommerening, C. A.; Sunderlin, L. S. *J. Phys, Chem. A* **1998**, *102*, 7674–7679.
(20) Artau, A.; Nizzi, K. E.; Hill, B. T.; Sunderlin, L. S.; Wenthold, P. G. *J. Am. Chem. Soc.* **2000**, *122*, 10667–10670.
(21) Crawford, E.; Mclndoe, J. S.; Tuck, D. G. *Can. J. Chem.* **2006**, *84*, 1607–1613.
(22) McIndoe, J. S.; Tuck, D. G. *Dalton Trans.* **2003**, *2*, 244–248.
(23) Nelson, I. V.; Iwamoto, R. T. *J. Electroanal. Chem.* **1964**, *7*, 218–221.
(24) Dorokhova, T. V.; Mikhailov, V. A.; Kanibolotskii, A. L.; Prokop'eva, T. M.; Savelova, V. A.; Popov, A. F. *Theor. Exp. Chem.* **2008**, *44*, 307–315.
(25) Trulove, P. C.; Osteryoung, R. A. *Inorg. Chem.* **1992**, *31*, 3980–3985.
(26) Campbell, J. L. E.; Johnson, K. E. *Inorg. Chem.* **1993**, *32*, 3809–3815.
(27) Zawodzinski, T. A., Jr.; Osteryoung, R. A. *Inorg. Chem.* **1988**, *27*, 4383–4384.
(28) Del Pópolo, M. G.; Kohanoff, J.; Lynden-Bell, R. M. *J. Phys. Chem. B* **2006**, *110*, 8798–8803.
(29) Pimentel, G. C. *J. Chem. Phys.* **1951**, *19*, 446–448.
(30) Ault, B. S.; Andrews, L. *J. Am. Chem. Soc.* **1975**, *97*, 3824–3826.
(31) Schreckenbach, G.; Ziegler, T. *J. Phys. Chem.* **1995**, *99*, 606–611.
(32) Schreckenbach, G.; Ziegler, T. *Int. J. Quantum Chem.* **1997**, *61*, 899–918.
(33) Wolff, S. K.; Ziegler, T. *J. Chem. Phys.* **1998**, *109*, 895–11.
(34) (a) te Velde, G.; Bickelhaupt, F. M.; van Gisbergen, S. J. A.; Guerra, C. F.; Baerends, E. J.; Snijders, J. G.; Ziegler, T. *J. Comput. Chem.* **2001**, *22*, 931. (b) Guerra, C. F.; Snijders, J. G.; te Velde, G.; Baerends, E. J. *Theor. Chem. Acc.* **1998**, *99*, 391. (c) ADF2007.01, SCM, *Theoretical Chemistry*, Vrije Universiteit, Amsterdam, The Netherlands, http://www.scm.com
(35) Wand, Y.; Li, H.; Han, S. *J. Chem. Phys.* **2005**, *123*, 174501–11.
(36) Dong, K.; Zhang, S.; Wang, D.; Yao, X. *J. Phys. Chem. A* **2006**, *110*, 9775–9782.
(37) Qiao, B.; Krekeler, C.; Berger, R.; Site, L. D.; Holm, C. *J. Phys. Chem. B* **2008**, *112*, 1743–1751.
(38) Bini, R.; Bortolini, O.; Chiappe, C.; Pieraccini, D.; Siciliano, T. *J. Phys. Chem. B* **2007**, *111*, 598–604.
(39) Chang, H. C.; Jiang, J. C.; Su, J. C.; Chang, C. Y.; Lin, S. H. *J. Phys. Chem. A* **2007**, *112*, 9201–9206.
(40) Bogaard, M. P.; Peterson, J.; Rae, A. D. *Acta Crystallogr., Sect. B* **1981**, *37*, 1357–1359.
(41) Lenoir, D.; Chiappe, C. *Chem.—Eur. J.* **2003**, *9*, 1036–1044.
(42) Ault, B. S.; Andrews, L. *J. Chem. Phys.* **1976**, *64*, 4853–4859.
(43) Waddington, T. C. *J. Chem. Soc.* **1958**, 1708–1709.
(44) Ault, B. S. *Acc. Chem. Res.* **1982**, *15*, 103–109.
(45) Kawaguchi, K. *J. Chem. Phys.* **1988**, *88*, 4186–4189.
(46) Melton, C. E.; Ropp, G. A.; Rudolph, P. S. *J. Chem. Phys.* **1958**, *29*, 968–969.